OMTM, Volume *29*

Supplemental information

Semi-automated workflows to quantify AAV transduction in various brain areas and predict gene editing outcome for neurological disorders

Fábio Duarte, Mergim Ramosaj, Ed Hasanovic, Sara Regio, Melanie Sipion, Maria Rey, and Nicole Déglon

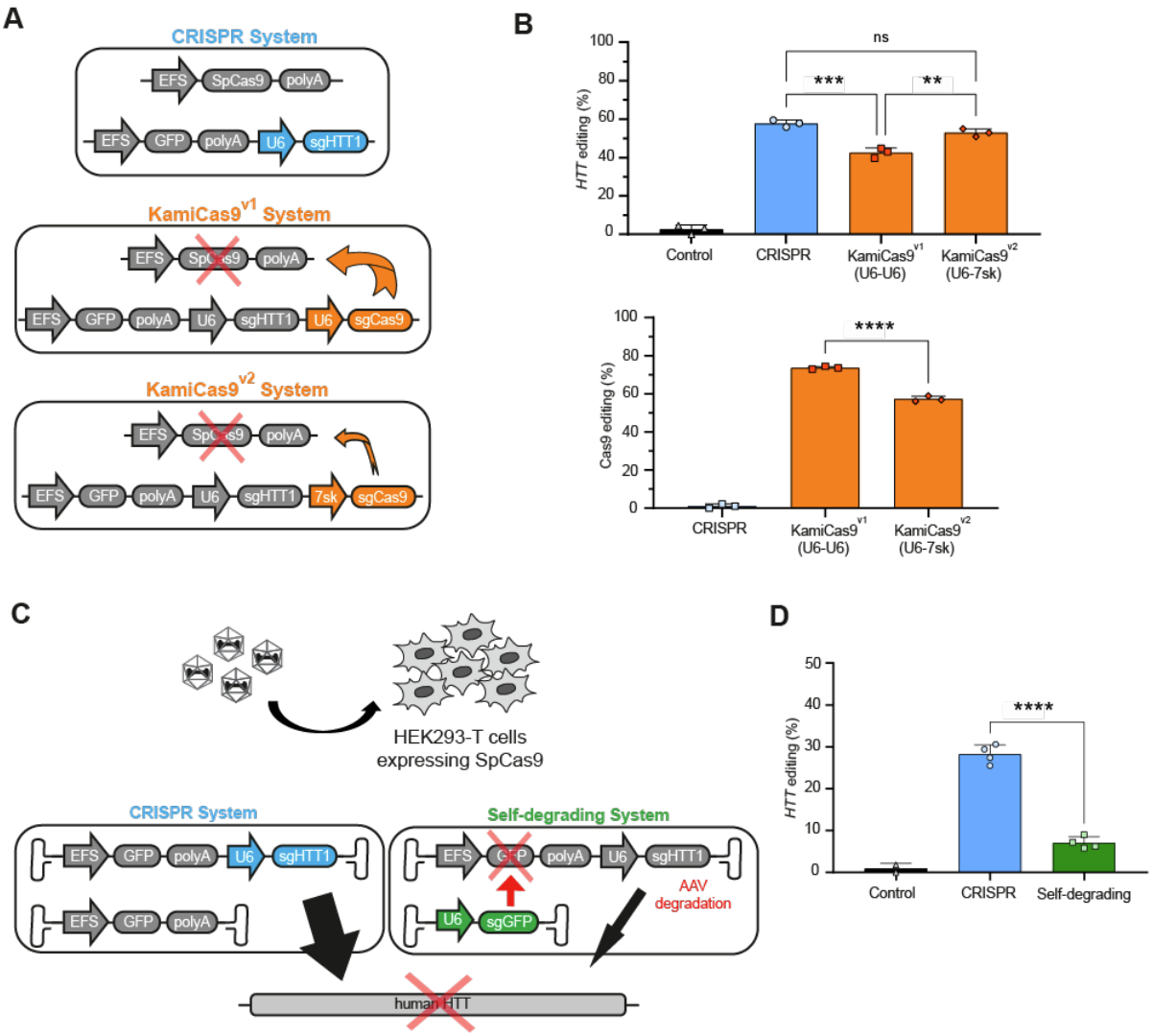

Figure S1. Characterization of the AAV-KamiCas9 system targeting the *HTT* gene in HEK293T cells, related to Figure 1. (A) Schematic representation of the CRISPR, KamiCas9^{v1} and KamiCas9^{v2} systems. All systems express a sgRNA targeting the translational start site of the human *HTT* gene (sgHTT1)[1] but the two KamiCas9 systems express an additional sgRNA targeting the translational start site of SpCas9 itself (sgCas9). The expression of sgCas9 is driven by the strong U6 promoter in the KamiCas9^{v1} system and by the weaker 7sk promoter in the KamiCas9^{v2} system. (B) The frequency of indels in the *HTT* and SpCas9 genes was assessed four days post-transfection, by TIDE[2] (*n*=3 replicates/group). (C) HEK293T cells stably expressing SpCas9 were transduced with AAV2/1 encoding the CRISPR system or a self-degrading system. The self-degrading system induces the cleavage of the AAV2/1 expressing the sgHTT1. (D) The *HTT* indel frequency measured by TIDE analysis seven days post-transduction showed that *HTT* editing levels were lower in the self-degrading group, suggesting that at least a fraction of cleaved AAV episomes are degraded (*n*=2 replicates for the control; *n*=4 replicates for CRISPR and the self-deleting system). Data are represented as mean ± SD.

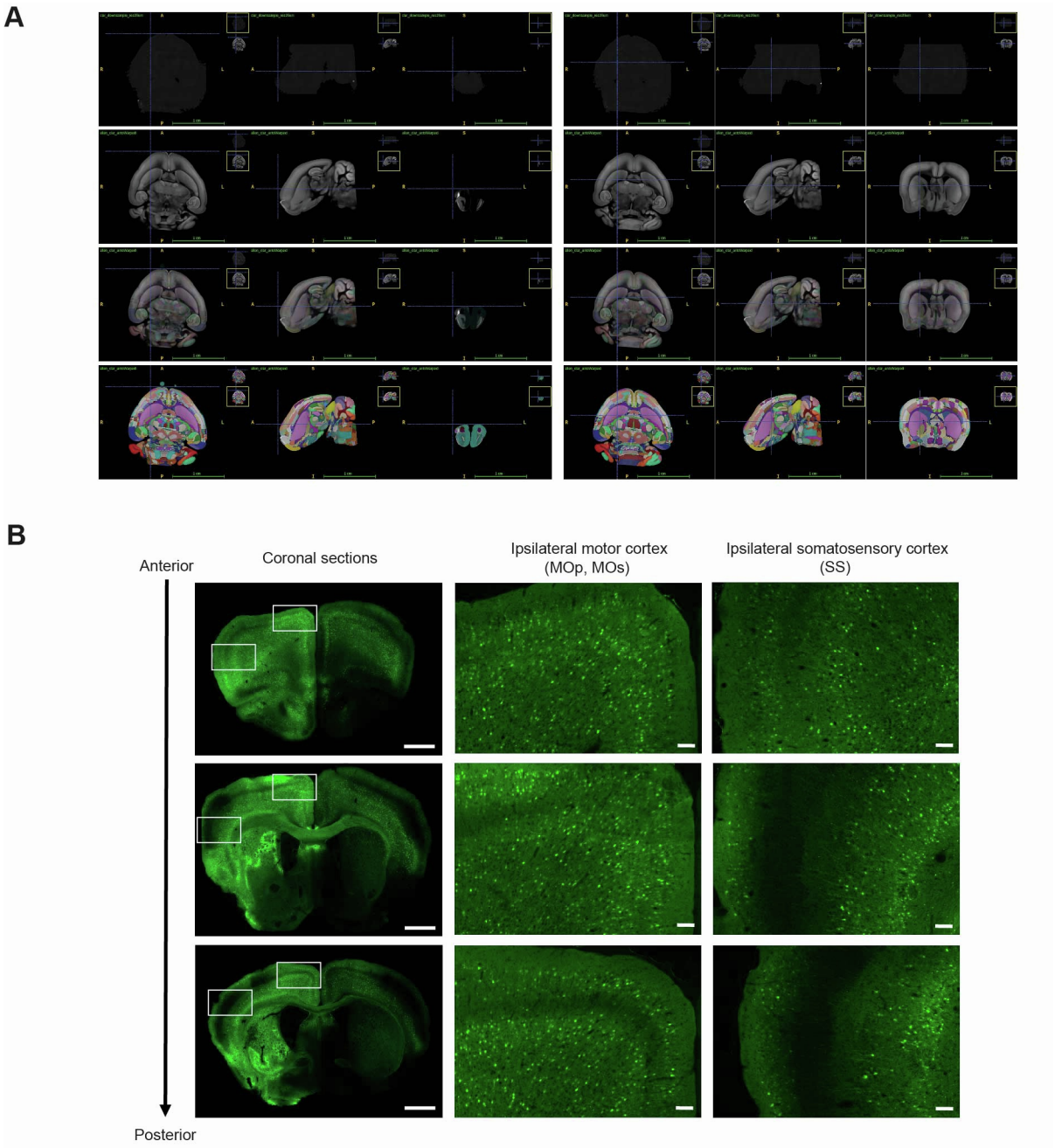
A
B
Anterior
Coronal sections
Ipsilateral motor cortex
(MOp, MOs)
Ipsilateral somatosensory cortex
(SS)
Posterior
C
Total number of cells
4'000'000
3'000'000
2'000'000
1'000'000
0
Blue Brain Cell Atlas
2D pipeline (DAPI+)
Frontal pole
(FRP)
Prelimbic area
(PL)
Orbital area
(ORB)
Anterior cingulate area
(ACA)
Infralimbic area
(ILA)
Somatomotor areas
(MOp and MOs)
Agranular insular area
(AI)
Gustatory area
(GU)
Retrosplenial area
(RSP)

Figure S2. Analysis of AAV2.retro transduction pattern following a unilateral intrastriatal injection, related to Figure 3. (A) The Allen CCFv3 reference atlas was deformed to fit the autofluorescence signals of dorso-ventral light sheet acquisitions of clarified brain (top) using the MIRACL pipeline. Lower panels show the progressive segmentation overlapped with difference transparency levels. (B) Rostro-caudal brain sections showing retrograde transport in the cortex and, in particular, massive transduction of the ipsilateral motor cortex (Mop, Mos) and, to a lesser extent, the somatosensory cortex (SS). Scale bar for low magnification: 1000 µm. Scale bar for high magnification: 100 µm. (C) Graph showing that the total number of cells in various cortical regions provided by the Blue brain atlas and the corresponding DAPI-positive cells identified with our 2D pipeline are is agreement.

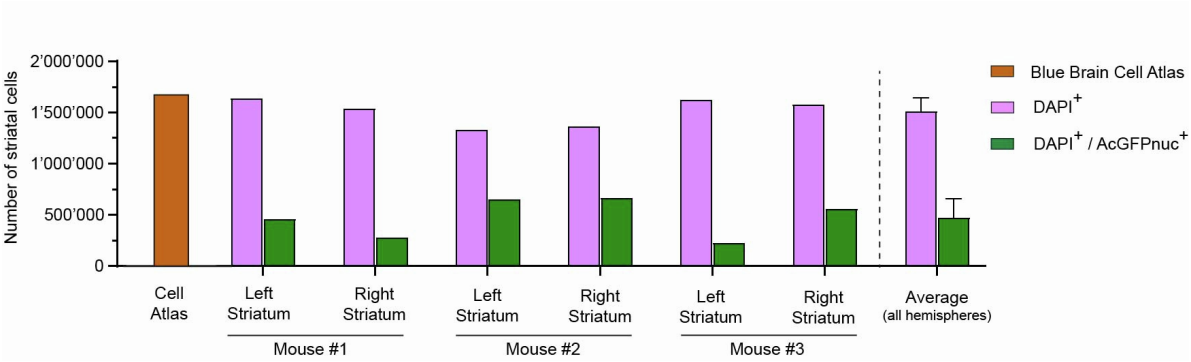

Figure S3. Quantification of the number of transduced cells in the striatum using the 2D pipeline, related to Figure 4. Graph showing the total number of striatal cells based on the Blue brain Cell Atlas, the corresponding number detected in the QuPath/Stardist analysis (DAPI staining) and finally the number of AcGFPnuc$^+$/DAPI$^+$ cells in the 3 animals analyzed. Data are represented as mean ± SD.

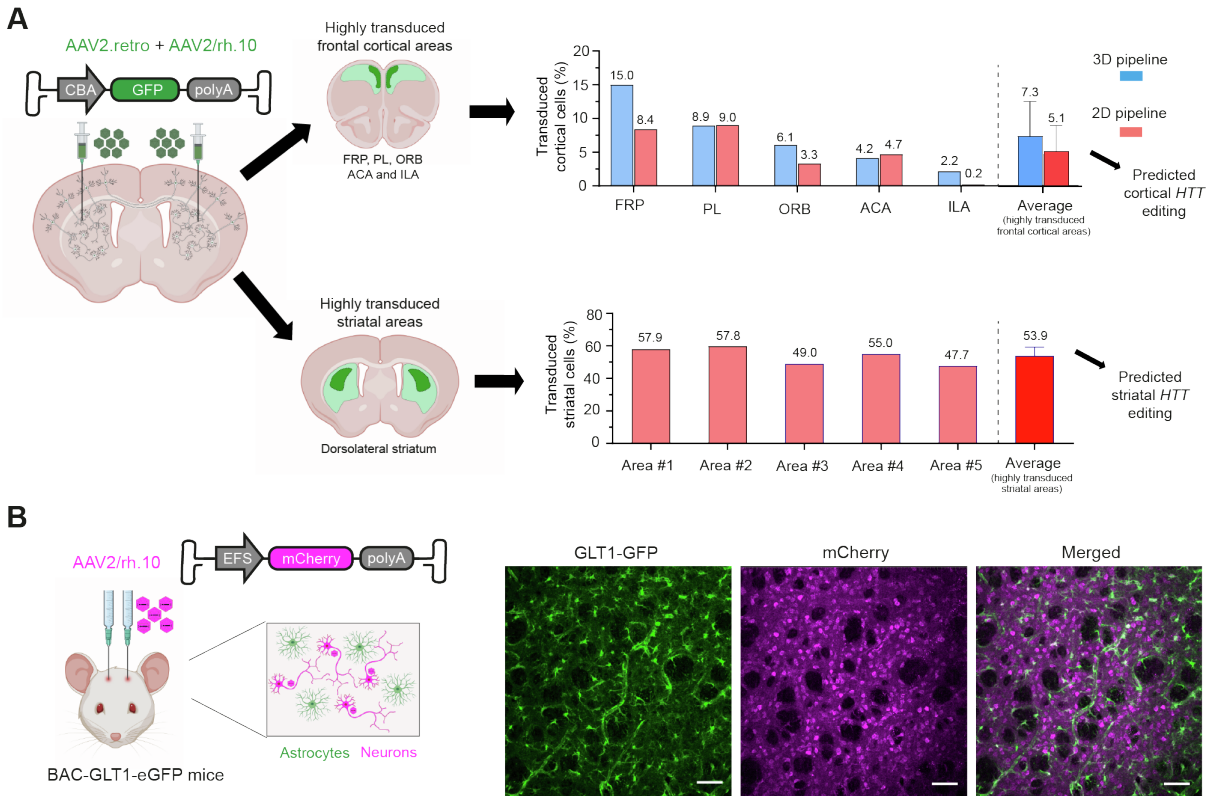

Figure S4. Prediction of HTT editing based on transduction efficiency and cell tropism, related to Figure 5. (A) For the *HTT* editing analysis, punch specimens were taken from the highly GFP-positive cortical and striatal areas. Because all cell types are present in the brain punches, we calculated the proportion of transduced cells over the total number of cells (neurons in Figure 3) at the most transduced areas to predict *HTT* editing outcome. Regarding the cortex, we focused on mediodorsal frontal cortical regions (including the FRP, PL, ORB, ACA, and ILA) as these were the areas with stronger GFP signal. Regarding the striatum, we used the previous quantification of the highly transduced striatal areas (Figure 4F). (B) The AAV2/rh.10 expressing mCherry under the control of EFS promoter was injected in BAC-GLT1-GFP transgenic mice. These mice endogenously express GFP in astrocytes. The poor localization between signals suggests that the AAV2/rh.10-EFS-mCherry (hence, AAV2/rh.10-EFS-SpCas9) has a strong neuronal tropism. Data are represented as mean ± SD.

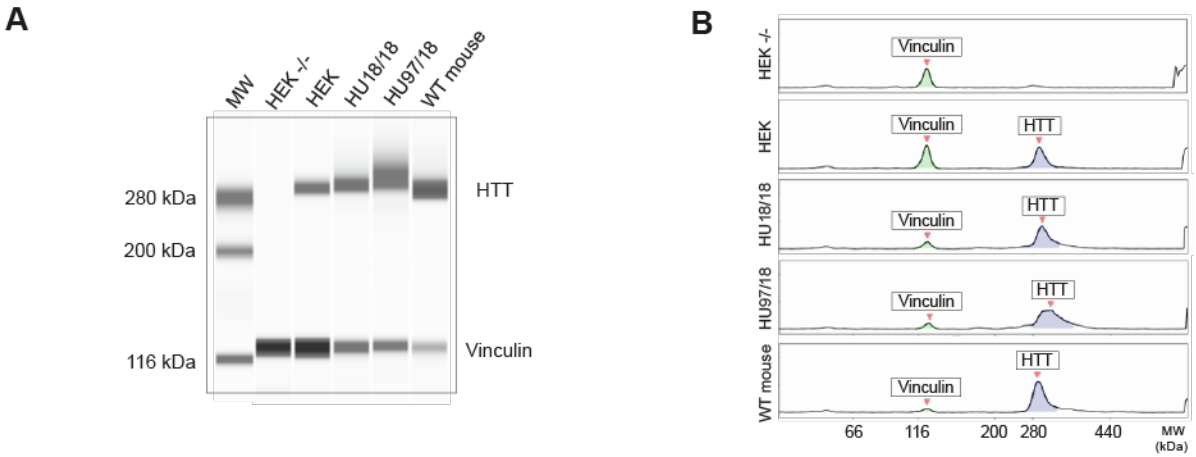

Figure S5. Validation of the capillary-based immunoassay for detecting HTT, related to Figure 5. (A) Validation of the immunoassay for the specific detection of HTT protein (4C8 antibody). Both mouse and human HTT proteins are detected by the 4C8 antibody. The selectivity of the signal was demonstrated in samples from $HTT^{-/-}$ HEK cells (knockout). The differences between samples for HTT protein migration were expected because HU97/18 mice express the mutant HTT with 97 CAG repeats. (B) Peak analysis with Compass software confirmed the specificity of the assay. The vinculin antibody was used as internal standard for the quantitative analysis.

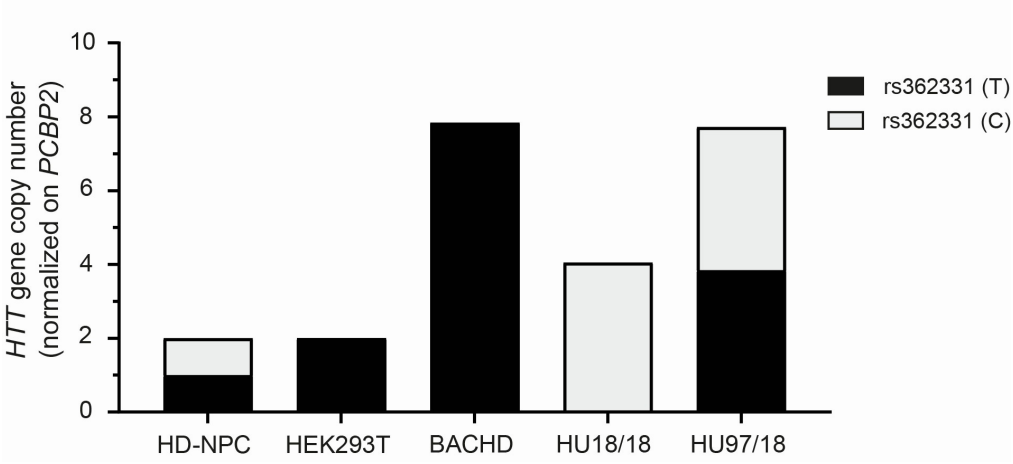

Figure S6. Absolute quantification of the HTT gene copy number by QIAcuity digital PCR, related to Figure 5. The HD transgenic mouse model HU97/18 is heterozygous for the SNP rs362331 (C/T) in the exon 50 of the HTT gene[3]. While the cytosine is linked to the *wtHTT* allele, the thymine is associated to the *mHTT* allele. Taqman assays with FAM/VIC probes targeting the SNP rs362331 (C/T) were used to determine the number of copies of *wtHTT* and *mHTT* alleles in HU97/18 mice. As a reference gene, we used the previously described Taqman assay targeting the poly(rC)-binding protein 2 (*PCBP2*) gene[4]. Genomic DNA from HD-derived neuronal precursor cells (HD-NPCs) was used to normalize quantifications as they are also heterozygous for the SNP rs362331 and contain two copies of the *HTT* gene (one *wtHTT* allele and one *mHTT* allele). Genomic DNA from HEK 293T cells were used to control copy number analysis since they are expected to have two *HTT* alleles. In addition, genomic DNA from BACHD and HU18/18 were used to control probe specificity because they are homozygous for the SNP rs362331.

Video S1. Processing of the 3D clarified brain for cell detection, related to Figure 3.

Video S2. Cell detection on the 3D clarified brain, related to Figure 3.

Table S1: Quantification of cortical AAV2.retro transduction with the 3D and 2D imaging workflows, **related to Figures 3 and S4.** Frontal pole (FRP), prelimbic area (PL), orbital area (ORB), anterior cingulate area (ACA), infralimbic area (ILA), primary and secondary somatomotor area (Mop, MOs), agranular insular area (AI), gustatory area (GU), restrosplenial area (RSP), somatosensory area (SS).

Brain Regions		Blue Brain Cell Atlas (BBCAv2)			3D Imaging workflow			2D Imaging workflow		
		Total cells (all layers)	Total excitatory neurons (Layers II/III, V and VI)	Targetable cells (%)	GFP+ cells	Transduction efficiency (%) (all layers)	Transduction efficiency (%) (excitatory neurons layers II/III, V and VI)	GFP+ cells	Transduction efficiency (%) (all layers)	Transduction efficiency (%) (excitatory neurons layers II/III, V and VI)
Isocortex		20'003'896	6'754'869	33.77	417'579	2.09	6.18	507'408	2.54	7.51
Isocortical Areas	Frontal pole (FRP)	28'248	8'225	29.12	4'233	14.99	51.47	2'368	8.38	28.79
	Prelimbic area (PL)	261'181	70'128	26.85	23'366	8.95	33.32	23'592	9.03	33.64
	Orbital area (ORB)	599'296	188'191	31.40	36'465	6.08	19.38	19'864	3.31	10.56
	Anterior cingulate area (ACA)	770'227	247'010	32.07	31'954	4.15	12.94	36'096	4.69	14.61
	Infralimbic area (ILA)	283'406	103'015	36.35	6'134	2.16	5.95	632	0.22	0.61
	Somatomotor areas (MOp and MOs)	2'927'777	646'633	22.09	181'718	6.21	28.10	174'936	5.98	27.05
	Agranular insular area (AI)	508'275	180'042	35.42	30'372	5.98	16.87	80'528	15.84	44.73
	Gustatory area (GU)	242'804	72'478	29.85	10'899	4.49	15.04	16'504	6.80	22.77
	Retrosplenial area RSP)	1'662'829	506'644	30.47	17'948	1.08	3.54	5'664	0.34	1.12
	Somatosensory areas (SS)	6'088'444	1'482'205	24.34	52'333	0.86	3.53	88'248	1.45	5.95
			AVERAGE	29.8	39’542	5.5	19.0	44’843	5.6	19.0
			AVERAGE (FRP, PL, ORB, ACA and ILA)	31.2	20’430	7.3	24.6	16’510	5.1	17.6

REFERENCES

1. Merienne, N., Vachey, G., de Longprez, L., Meunier, C., Zimmer, V., Perriard, G., Canales, M., Mathias, A., Herrgott, L., Beltraminelli, T., et al. (2017). The Self-Inactivating KamiCas9 System for the Editing of CNS Disease Genes. Cell Rep *20*, 2980–2991.
2. Brinkman, E.K., Chen, T., Amendola, M., & van Steensel, B. (2014). Easy quantitative assessment of genome editing by sequence trace decomposition. Nucleic Acids Res *42*, 168.
3. Southwell, A.L., Warby, S.C., Carroll, J.B., Doty, C.N., Skotte, N.H., Zhang, W., Villanueva, E.B., Kovalik, V., Xie, Y., Pouladi, M.A., et al. (2013). A fully humanized transgenic mouse model of Huntington disease. Hum Mol Genet *22*, 18–34.
4. Christodoulou, I., Patsali, P., Stephanou, C., Antoniou, M., Kleanthous, M., & Lederer, C.W. (2016). Measurement of lentiviral vector titre and copy number by cross-species duplex quantitative PCR. Gene Ther *23*, 113–118.